Am J Physiol Cell Physiol
281: C1604–C1613, 2001.

Opposing gates model for voltage gating of gap junction channels

YE CHEN-IZU,[1] ALONSO P. MORENO,[2] AND ROBERT A. SPANGLER[3]
[1]*Department of Physiology, University of Maryland School of Medicine, Baltimore, Maryland 21201;* [2]*Department of Medicine, Krannert Institute of Cardiology, Indianapolis, Indiana 46202; and* [3]*Department of Physiology and Biophysics, State University of New York at Buffalo, Buffalo, New York 14214*

Received 1 February 2001; accepted in final form 11 July 2001

Chen-Izu, Ye, Alonso P. Moreno, and Robert A. Spangler. Opposing gates model for voltage gating of gap junction channels. *Am J Physiol Cell Physiol* 281: C1604–C1613, 2001.—Gap junctions are intercellular channels that link the cytoplasm of neighboring cells. Because a gap junction channel is composed of two connexons docking head-to-head with each other, the channel voltage-gating profile is symmetrical for homotypic channels made of two identical connexons (hemichannels) and asymmetric for the heterotypic channels made of two different connexons (i.e., different connexin composition). In this study we have developed a gating model that allows quantitative characterization of the voltage gating of homotypic and heterotypic channels. This model differs from the present model in use by integrating, rather than separating, the contributions of the voltage gates of the two member connexons. The gating profile can now be fitted over the entire voltage range, eliminating the previous need for data splicing and fusion of two hemichannel descriptions, which is problematic when dealing with heterotypic channels. This model also provides a practical formula to render quantitative several previously qualitative concepts, including a similarity principle for matching a voltage gate to its host connexon, assignment of gating polarity to a connexon, and the effect of docking interactions between two member connexons in an intact gap junction channel.

connexin; cell signaling; mathematical model

GAP JUNCTIONS ARE INTERCELLULAR channels that directly link the cytoplasm of adjacent cells. Cell-cell communication via gap junctions has been recognized to play important roles in many physiological processes, such as impulse propagation in the heart and neurons, nutrient supply in the lens, pattern formation during development, and regulation of cell growth and transformation (for reviews see Refs. 3, 5, 25, and 27). The gap junction channels also provide a unique system for the study of structure-function relationships of protein molecules, because their structure is unique among ion channels. A gap junction channel is composed of two connexons that protrude from two neighboring cells and dock with each other via their extracellular loops (13, 32). Each connexon is made of 6 connexin subunits, of which 18 different isoforms have been identified and cloned. Each connexin forms channels with distinctive properties, including single-channel conductance (33), channel permeability (9, 12, 14), gating response to pH (18, 19), and voltage-sensitive gating (22). Gap junction voltage gating is the most extensively characterized fingerprint for channels made of various connexin types. Because the two connexons that constitute a gap junction are oriented as mirror images of each other in an intact channel, a homotypic channel made of two identical connexons has a symmetrical structure (32), whereas a heterotypic channel made of two different connexons has an asymmetric structure. Consequently, the channel voltage-gating profile, which is the relationship between channel conductance and transjunctional voltage (V_j), is largely symmetrical for homotypic channels across positive and negative voltage ranges but asymmetric for heterotypic channels.

Alterations in channel protein structure, by molecular techniques or by pairing connexons in various combinations, often lead to changes in the channel voltage gating (24, 26, 30, 34). To study the structure-function relationship, Spray, Harris, and Bennett (15, 28) developed a quantitative (S-H-B) model for the channel voltage gating, in which a single Boltzmann function was used to characterize a symmetrical voltage-gating profile. Later, use of the S-H-B model was extended to also describe the asymmetric gating of heterotypic channels. The common practice is to splice the voltage-gating profiles into two segments in the positive and negative voltage (V_j) ranges or at the V_j of peak conductance (17, 20, 22, 26, 34, 37). Each of the two data segments is then fitted to a single Boltzmann function. In the case of the homotypic channels that are fully open at $V_j = 0$ mV, each connexon contributes to one-half of the voltage-gating profile, so it is reasonable to splice the gating profile at $V_j = 0$ mV. However, if the gating profiles of two connexons overlap, with a voltage range in which neither connexon is fully conducting, the contributions of two member connexons are integrated and, therefore, cannot be separated at $V_j = 0$

Address for reprint requests and other correspondence: Y. Chen-Izu, Dept. of Physiology, University of Maryland School of Medicine, 655 W. Baltimore St., Baltimore, MD 21201-1559 (E-mail: ychen005@umaryland.edu).

The costs of publication of this article were defrayed in part by the payment of page charges. The article must therefore be hereby marked "*advertisement*" in accordance with 18 U.S.C. Section 1734 solely to indicate this fact.

mV. It is equally arbitrary to separate the gating profile of a heterotypic channel at the V_j of peak conductance. Moreover, when the gating profile is spliced to two segments and each is fitted independently to a single Boltzmann function, the intersection of the two fitting curves often produces an odd point with a discontinuous first derivative that clearly does not reflect a physical reality. This discontinuity reveals the problem inherent in the practice of adapting the S-H-B model to heterotypic channels. Recently, Vogel and Weingart (35) presented a detailed model using four conductance states and two voltage gates to describe an intact gap junction channel. Their model included many variations that could arise in gap junction conduction. However, because their mathematical description was given in general form (consisting of ≥13 free parameters), it does not provide a practical formula to characterize the real experimental data of macroscopic currents.

Here we present a simple four-state model to integrate the contribution of the two member connexons in an intact gap junction channel. This model employs three new considerations: *1*) thermodynamic self-consistency in the Gibbs free energy of the system, *2*) assumption of one open channel conductance and one residual conductance value for an intact channel, and *3*) simplification afforded by assuming independent or contingent gating. [This assumption was first proposed by Spray et al. (29); here we translate it into a new mathematical formula.] This model provides a practical formalism for fitting the experimental data of macroscopic currents over the entire voltage range in the voltage-gating profile, eliminating the need for arbitrary data splicing and fusion of two hemichannel descriptions. The model also helps to render several previously qualitative concepts in quantitative terms, particularly those relating to matching a voltage gate to its host connexon and defining the docking interaction between two hemichannels.

METHODS

Expression of gap junctions composed of homotypic and heterotypic connexins. The experimental data used here for model fitting were previously published, and the methods used in obtaining these data have been described elsewhere (see footnotes in Table 1). Connexin30 (Cx30), connexin26 (Cx26), and connexin32 (Cx32) were expressed in *Xenopus* oocytes (11); connexin43 (Cx43) and connexin45 (Cx45) were expressed in N2A cells (20). Briefly, when *Xenopus* oocytes are used to express connexin cRNAs, the endogenous connexin38 (Cx38) is first suppressed by preinjection with an antisense oligonucleotide to the 5′ end of *Xenopus* Cx38 3–4 days before injection with exogenous connexin RNA, as previously described (2). The follicular membranes of the oocytes were removed before injection. The inner vitelline membranes were removed 1 day after the injection of RNA, and the oocytes were paired in an agar well to force close contact with each other. Gap junction conductance between paired oocytes was measured after 24–48 h of incubation at room temperature. The oocytes were maintained in L-15 medium (GIBCO). The solution was changed twice per day to prevent contamination.

The connexin RNA was prepared using the in vitro transcription methods previously described (2). The integrity of synthesized RNA was verified by agarose gel electrophoresis. The concentration of the RNA was estimated by ultraviolet absorption at 260 nm, with purity assessed by the 260 nm-to-280 nm ratio.

Dual-cell voltage clamp. The experiments on the gap junctions expressed in *Xenopus* oocytes were performed on an electrophysiology setup containing the following instruments: two Geneclamp500 amplifiers, a Digidata 1200 analog-to-digital converter, a VA-100 analog-to-digital recorder, a JVC video recorder, and a personal computer. pClamp6 (Axon Instrument) was used for data acquisition. Dual-cell voltage-clamp techniques were used to measure the gap junction coupling between cell pairs. To increase input resistance of cells, micropipettes were filled with a patch solution containing cesium (130 mM CsCl, 0.5 mM $CaCl_2$, 10 mM HEPES, 10 mM EGTA, pH 7.2). During recording, cells were kept at room temperature in a cesium-containing solution (160 mM NaCl, 7 mM CsCl, 2.0 mM $CaCl_2$, 0.6 mM $MgCl_2$, 10 mM HEPES, pH 7.4). The cells in a pair, *cell L* and *cell R*, were individually voltage clamped. The holding potential for both cells was −60 mV, close to the cell resting potential. V_j steps were delivered to *cell R*, while the voltage was held constant in *cell L*. The evoked current in *cell L* was then recorded as the transjunctional current.

Data analysis. We used pClamp6, Excel (Microsoft), and Prism (GraphPad Software) for data analysis. The current decay due to voltage gating was best fitted to exponential functions. The initial current was then obtained by extrapolation to *time 0*; the steady-state current was obtained as the offset of the exponential fitting at infinity. V_j was obtained as the potential difference between the two voltage electrodes. The initial conductance (G_i) and the steady-state conductance (G_{ss}) were calculated from the initial and the steady-state current, respectively, as the ratio of current to voltage. In plotting the relationship between conductance and voltage, the sign of V_j is referenced to the cytoplasmic side of CxR in a connexon pair denoted CxL/CxR (CxL in *cell L*; CxR in *cell R*).

RESULTS

Voltage gating of gap junctions. A homotypic gap junction channel made of two identical connexons has a largely symmetrical voltage-gating profile. Figure 1*A* shows the currents through homotypic Cx30 channels evoked by V_j steps from −105 to +105 mV in 10-mV increments (published initially in Ref. 11). The currents are largely symmetrical for positive and negative voltage ranges. The currents reach an initial maximum and then decay to a steady-state level during the maintained voltage step, revealing the voltage-gating phenomenon. We calculated G_i and G_{ss} from the current-voltage relationship and normalized the G_i and G_{ss} of each cell pair to the interpolated value of its G_i at V_j = 0 mV, so that data from cell pairs with different coupling levels can be compared. Predictably, homotypic gap junctions, such as those composed exclusively of Cx30, exhibit a symmetrical gating profile (Fig. 1*B*).

A heterotypic channel made of two different connexons often has an asymmetric gating profile. Figure 1*C* shows the currents through heterotypic Cx30/Cx32 channels, which present a dramatic asymmetry in the

Table 1. *Gap junction voltage-gating parameters and docking interaction between connexon pairs*

Connexon Pairing (CxL/CxR)	Gate$_{-V}$		Gate$_{+V}$					Gate CxL		Gate CxR		
	A_1, mV^{-1}	V_{o1}, mV	A_2, mV^{-1}	V_{o2}, mV	g_{res}	g_{max}	$P_{o,i}$	Q, e	U_o, meV	Q, e	U_o, meV	Polarity (CxL/CxR)
Homotypic Cx30/Cx30	0.116	41.5	0.116	41.5	0.25	1.00	1.0	3.0	125	3.0	125	+
Homotypic Cx32/Cx32	0.114	56.0	0.114	56.0	0.31	1.00	1.0	−2.9	165	−2.9	165	−
Heterotypic Cx30/Cx32	0.106	59.0	Masked	Masked	0.38	1.00	1.0	Masked	Masked	−2.7	161	+/−
Docking ΔCx30/ΔCx32								Masked	Masked	0.2	−4	
Homotypic Cx40/Cx40	0.309	34.6	0.309	34.6	0.20	1.00	1.0	8.0	276	8.0	276	+
Homotypic Cx37/Cx37	0.259	16.5	0.259	16.5	0.26	1.07	0.9	6.7	110	6.7	110	+
Heterotypic Cx40/Cx37	0.407	26.3	0.245	19.5	0.28	1.02	1.0	10.5	277	6.3	124	+/+
Docking ΔCx40/ΔCx37								2.5	1	−0.4	13	
Homotypic Cx43/Cx43	0.058	61.3	0.058	61.3	0.29	1.00	1.0	−1.5	92	−1.5	92	−
Homotypic Cx45/Cx45	0.110	10.2	0.110	10.2	0.06	1.56	0.6	−2.8	29	−2.8	29	−
Heterotypic Cx43/Cx45	0.088	22.3	0.027	125.3	0.04	1.03	1.0	−0.7	89	−2.3	51	−/−
Docking ΔCx43/ΔCx45								0.8	−3	0.6	22	
Homotypic Cx30/Cx30	0.116	41.5	0.116	41.5	0.25	1.00	1.0	3.0	125	3.0	125	+
Homotypic Cx26/Cx26	0.101	95.2	0.101	95.2	0.11	1.00	1.0	2.6	248	2.6	248	+
Heterotypic Cx30/Cx26	0.153	59.8	N/D	N/D	0.28	1.06	0.9	3.9	236	N/D	N/D	+/+
Docking ΔCx30/ΔCx26								0.9	111	N/D	N/D	
Homotypic Cx26/Cx26	0.101	95.2	0.101	95.2	0.11	1.00	1.0	2.6	248	2.6	248	+
Homotypic Cx30.3β/Cx30.3β	0.062	79.6	0.062	79.6	0.15	1.00	1.0	1.6	129	1.6	129	+
Heterotypic Cx26/Cx30.3β	0.161	74.5	0.096	58.9	0.15	1.00	1.0	4.2	310	2.5	146	+/+
Docking ΔCx26/ΔCx30.3β								1.6	62	0.9	18	
Homotypic Cx26/Cx26	0.101	95.2	0.101	95.2	0.11	1.00	1.0	2.6	248	2.6	248	+
Homotypic Cx50/Cx50	0.199	25.2	0.199	25.2	0.12	1.04	1.0	5.2	130	5.2	130	+
Heterotypic Cx26/Cx50	0.160	58.2	0.166	48.2	0.19	1.00	1.0	4.1	241	4.3	207	+/+
Docking ΔCx26/ΔCx50								1.5	−7	−0.9	77	

Sources of experimental data used in the above model fitting are as follows: Dahl et al. (11) for gap junctions made of Cx30, Cx26, and Cx32 combinations, Hennemann et al. (17) for gap junctions made of Cx37 and Cx40 combinations, Moreno et al. (20) for gap junctions made of Cx43 and Cx45 combinations, and Zhu and Nicholson (personal communication) for gap junctions made of Cx26, Cx30.3β, and Cx50 combinations. CxL/CxR, connexons at left side and right side, respectively; gate$_{-V}$ and gate$_{+V}$, parameters of the gate that closes at a negative and positive voltage (relative to CxR side), respectively; g_{res} and g_{max}, normalized residual and maximum conductances, normalized to initial conductance; $P_{o,i}$, calculated channel open probability at initial moment (*Eq. 14*). Gating charge (Q) and transition energy between open and closed states (U_o) calculated from voltage sensitivity coefficient (A) and voltage for half-maximal conductance (V_o) values for each gate (*Eqs. 12* and *13*) are used to assign each gate to a specific connexon by comparing the 2 gates in the heterotypic channel with the reference values of the 2 member connexons. Polarity, gating polarity of each connexon, corresponding to the sign of Q assigned to it. N/D, not determined.

voltage-gating profile (Fig. 1*D*). Stepping to negative voltages greater than −40 mV evoked large currents that decayed to smaller steady-state currents over time; stepping to more positive voltages evoked much smaller currents that showed little decay. This marked rectification of G_i in the gating profile is similar to that reported in heterotypic pairings of Cx32 with other connexons, e.g., Cx26/Cx32 (2), Cx46/Cx32, and Cx50/Cx32 (37).

The voltage dependence of G_i should reflect, in principle, the voltage dependence of the single-channel conductance, because the initial open probability ($P_{o,i}$) is a constant value, fixed by the holding potential (0 mV in most experiments). The voltage dependence of G_{ss}, however, is determined not only by single-channel conductance, but also by changes in the channel open probability (P_o) due to voltage gating. The present study is focused on modeling this steady-state voltage gating of homotypic and heterotypic gap junction channels.

Opposing gates model for gap junction voltage gating. Our model assumes that each member connexon contributes one voltage gate, and therefore two voltage gates in series control the gating of an intact gap junction channel. The schematic presentation of the model is shown as

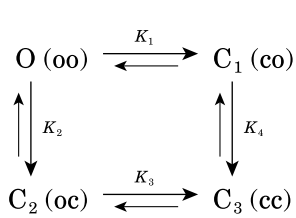

where K_i (i = 1, 2, 3, 4) is the equilibrium constant for each of the transition processes, with the forward transition taken in the direction indicated by the long arrows. A channel can occupy one of the four possible states: *1*) O(oo), in which both gates are open, *2*) C_1(co), in which *gate L* is closed and *gate R* is open, *3*) C_2(oc), in which *gate L* is open and *gate R* is closed, and *4*) C_3(cc), in which both gates are closed. An identical four-state

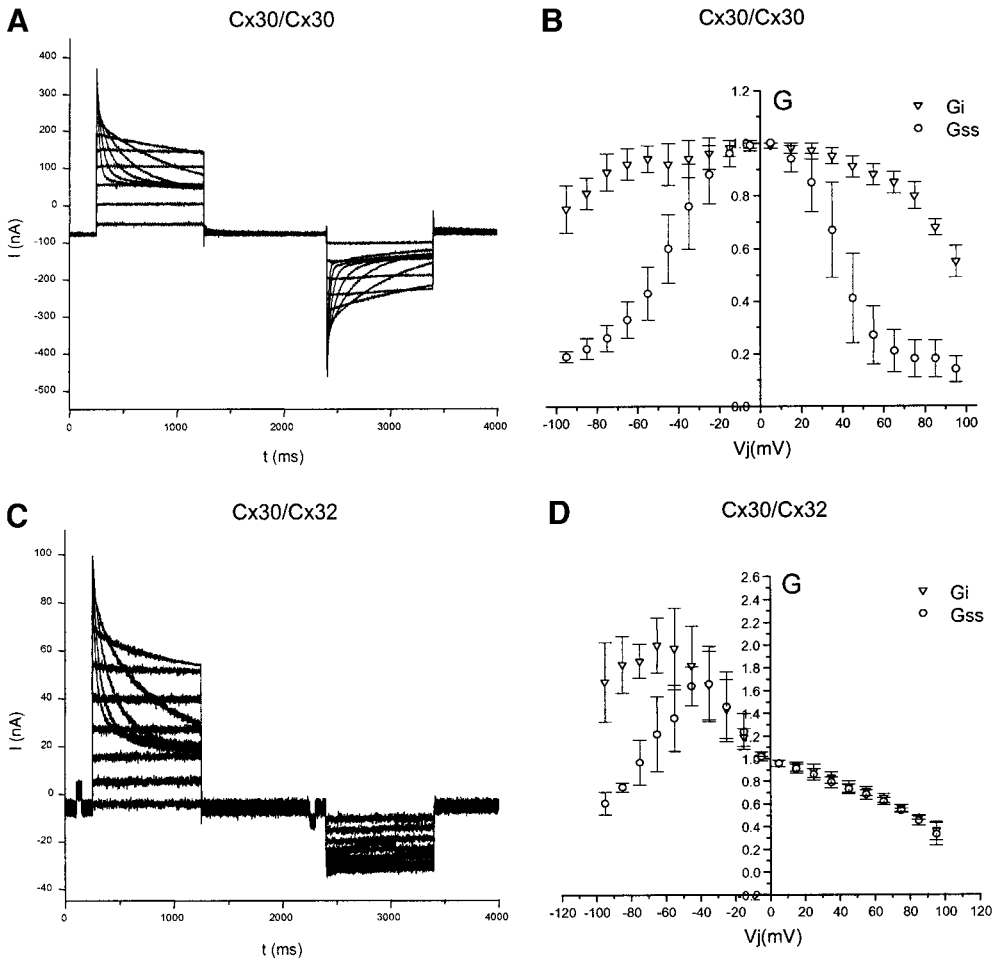

Fig. 1. Transjunctional currents and conductance of gap junction channels. *A*: macroscopic currents through homotypic Cx30/Cx30 channels, evoked by transjunctional voltage (V_j) steps from −105 to +105 mV in 10-mV increments from a holding potential of 0 mV. Both cells were held at −60 mV at resting condition. Cx, connexin; *I*, current; *t*, time. *B*: relationship between averaged channel conductance and V_j of Cx30/Cx30 channel (17 cell pairs). This channel has a largely symmetrical voltage-gating profile. G_i, initial conductance; G_{ss}, steady-state conductance. *C*: macroscopic currents through heterotypic Cx30/Cx32 channels evoked by the same voltage-clamp protocol used in *A*. *D*: relationship between averaged channel conductance and V_j of heterotypic Cx30/Cx32 channel (21 cell pairs). Cx30/Cx32 channel has a distinctively asymmetric voltage-gating profile.

scheme was proposed conceptually by Moreno et al. (21), put into a mathematical expression (10, 23), and incorporated into a general model (35). Here we develop this four-state scheme into a circumscribed mathematical model by utilizing three considerations: *1*) detailed balance of the state transitions, *2*) separation of P_o from the macroscopic conductance, and *3*) assumption of independent/contingent gating.

The equilibrium constants between the states can be expressed explicitly in terms of V_j or V (the subscript j is dropped to simplify notation) as a Boltzmann relation

$$\begin{aligned} K_1 &= e^{A_1 \cdot (-V - V_{o1})} \\ K_2 &= e^{A_2 \cdot (V - V_{o2})} \\ K_3 &= e^{A_3 \cdot (-V - V_{o3})} \\ K_4 &= e^{A_4 \cdot (V - V_{o4})} \end{aligned} \qquad (1)$$

where A_i is the voltage sensitivity coefficient and V_{oi} is the voltage for half-maximal conductance. The sign for V is negative for K_1 and K_3 but positive for K_2 and K_4, because the two voltage gates are oriented as mirror images of each other.

Fundamental thermodynamic considerations, based on the consistency of free energy change between any two states regardless of the pathway, require that $K_1 \cdot K_4 = K_2 \cdot K_3$. Under this constraint, the probability of a gap junction channel being open (P_o) can be calculated from the equilibrium distribution among the available states

$$P_o = \frac{O}{O + C_1 + C_2 + C_3} = \frac{1}{1 + K_1 + K_2 + K_1 \cdot K_4} \qquad (2)$$

If it is assumed that the channel displays a single-channel conductance level in the open state, the relationship between the conductance of a population of gap junction channels and the steady-state P_o is

$$P_o = \frac{G_{ss} - G_{min}}{G_{max} - G_{min}} \qquad (3)$$

where G_{max} is the maximum conductance, G_{ss} is the steady-state conductance, and G_{min} is the minimum conductance (equivalent to *Eq. 5* in Ref. 28). To characterize the voltage gating, we isolate P_o from the other two factors, namely, single-channel conductance and total number of channels, by taking a ratio of the above conductance to the initial conductance. This produces

$$P_o = \frac{g_n - g_{res}}{g_{max} - g_{res}} \qquad (4)$$

where $g_n = G_{ss}/G_i$ is the normalized steady-state conductance, $g_{max} = G_{max}/G_i$ is the normalized maximum

conductance, and $g_{res} = G_{min}/G_i$ is the normalized residual conductance. G_i denotes the initial conductance or instantaneous conductance. By definition, $g_{max} \geq 1$ and $0 \leq g_{res} \leq 1$. G_i might be smaller than G_{max} if some channels are not open at the initial moment. The g_{res} reflects a persistent conductance in the closed state that is present in most gap junction channels studied, unless the channels are closed by phosphorylation or pathological pH (7, 21). With rearrangement, we obtain the following equation

$$g_n = g_{res} + (g_{max} - g_{res}) \cdot P_o \quad (5)$$

The above treatment is based on a simplifying assumption that an intact gap junction channel has one open channel conductance and one residual conductance. A more complicated scheme includes one open channel conductance and one residual conductance for each connexon (hemichannel), giving rise to four possible conductances corresponding to the four kinetic states for an intact channel (35).

Multiple single-channel conductances, as determined by single-channel patch-clamp techniques, have been reported in several gap junction channels (6, 21, 31). Nonetheless, the available experimental data concerning macroscopic currents do not have sufficient resolution to allow us to distinguish between the available models (as demonstrated later in regard to the independent vs. the contingent model). As a practical matter, we use the above simplifying assumption to extend from the original S-H-B model (15, 28) and, at the same time, to avoid the complications in the general model (35) that cannot be resolved by the experimental data of macroscopic currents. Although it is relatively simple, this four-state equilibrium model can accommodate a number of rather complex features that can arise in gap junctions. For example, direct interaction between the connexons, such that the P_o of one gate depends on the state of the other, would be represented quite simply by a difference between the appropriate K values, e.g., K_1 and K_3. On the other hand, an indirect effect mediated by changes in the electrical potential profile across the connexon pair would be modeled by a difference in A in the exponential expressions for the equilibrium constants.

Contingent gating model. On the basis of the physical considerations originally proposed by Harris et al. (15), we further simplify the above scheme to two specific models. The contingent gating model assumes that if one gate is closed, the other gate must be open. The underlying consideration is that V_j would drop entirely across the closed gate, so there would be no voltage drop across the open gate. This assumption, together with the assumption that a gate has negligible probability of closing in the absence of a voltage drop across it, leads to $K_3 = K_4 = 0$. Under these conditions, we have

$$P_o = \frac{1}{(1 + K_1 + K_2)} = 1/[1 + e^{A_1(-V - V_{o1})} + e^{A_2(V - V_{o2})}] \quad (6)$$

Thus we obtain the following equation for the contingent model

$$g_n = g_{res} + \frac{g_{max} - g_{res}}{1 + e^{A_1(-V - V_{o1})} + e^{A_2(V - V_{o2})}} \quad (7)$$

Equation 7 contains six free parameters: A_1, A_2, V_{o1}, V_{o2}, g_{res}, and g_{max}. In the case of a homotypic channel with two identical gates, we have the constraint $A_1 = A_2$ and $V_{o1} = V_{o2}$, so the free parameters are reduced to four. Thus, for homotypic channels, we have

$$g_n = g_{res} + \frac{g_{max} - g_{res}}{1 + e^{A(-V - V_o)} + e^{A(V - V_o)}} \quad (8)$$

Independent gating model. The independent gating model assumes that the two voltage gates in a gap junction channel do not influence each other, through direct interaction or indirectly through changes in the distribution of V_j over the two hemichannels. Hence, the probability of one gate being open is independent of the state of the other. This assumption leads to $K_1 = K_3$ and $K_2 = K_4$. Under these conditions

$$P_o = \frac{1}{(1 + K_1) \cdot (1 + K_2)} = 1/[1 + e^{A_1 \cdot (-V - V_{o1})}] \cdot [1 + e^{A_2(V - V_{o2})}] \quad (9)$$

Thus we obtain the following equation for the independent gating model

$$g_n = g_{res} + \frac{g_{max} - g_{res}}{[1 + e^{A_1(-V - V_{o1})}] \cdot [1 + e^{A_2(V - V_{o2})}]} \quad (10)$$

Equation 10 also contains six free parameters, A_1, A_2, V_{o1}, V_{o2}, g_{res}, and g_{max}, for heterotypic channels. For a homotypic channel, the free parameters are reduced to four, and we have

$$g_n = g_{res} + \frac{g_{max} - g_{res}}{[1 + e^{A(-V - V_o)}] \cdot [1 + e^{A(V - V_o)}]} \quad (11)$$

For a homotypic channel, the model equations of contingent and independent models become even functions of voltage, $g_n(V) = g_n(-V)$, because of the constraint $A_1 = A_2$ and $V_{o1} = V_{o2}$. This symmetry in the model equations concurs with the symmetrical gating of homotypic channels.

Voltage-gating parameters. The parameters A and V_o in the above-mentioned models describe the gap junction channel voltage gating in terms of the voltage sensitivity and the half-maximal voltage. However, to relate these functional measures to the underlying molecular structure, it is preferable to convert these descriptive parameters to physical terms. If we view voltage gating as being controlled by a charge movement, or a dipole rotation, in the channel molecule, the gating can be characterized by the equivalent gating charge (Q) and the transition energy between open and closed states (U_o). Q and U_o are related to A and V_o as follows

$$Q = kT \cdot A \quad (12)$$

$$U_o = kT \cdot A \cdot V_o \quad (13)$$

We use the elementary charge (e) for the unit of Q and millielectron volts (meV) for the unit of U_o. Q is calculated as the equivalent net charge involved in the voltage gating, with the assumption that these charges move across the entire transjunctional electrical field. To relate Q to the number of charged and polar residues in the channel molecule, one needs to consider that voltage gating could involve translocation of positive and/or negative charges and/or dipole rotation across only a fraction of the potential field because of structural constraints. Hence, the actual charge involved in gating is probably larger than Q. During a voltage pulse, external energy input $U(V)$ causes a shift in the gating state. If $U > U_o$, the gate becomes more likely to be in the closed rather than the open state. Conversely, for $U < U_o$, the gate is predominantly open.

The normalized residual conductance, $g_{res} = (G_{min}/G_i) \leq 1$, reflects the remaining conductance when the voltage gates are closed, usually under high voltages. For homotypic channels, the residual conductance has the same value at the positive and negative voltages. For heterotypic channels, the residual conductance could have two different values. However, in known cases such as heterotypic Cx37/Cx40 (17), Cx26/Cx50, and Cx26/Cx30.3β (Zhu and Nicholson, personal communication), the residual conductance values at the positive and negative voltages are similar. In this model we have made the simplifying assumption that there is only one g_{res} value for an intact channel.

The normalized maximum conductance gives the ratio of maximum conductance to initial conductance, $g_{max} = (G_{max}/G_i) \geq 1$. If $g_{max} = 1$, all the channels are open at the initial moment of the voltage step. If $g_{max} > 1$, some channels are closed. The P_o at the initial moment ($P_{o,i}$) can be calculated from the g_{res} and g_{max} as follows

$$P_{o,i} = \frac{1 - g_{res}}{g_{max} - g_{res}} \quad (14)$$

Example of using the model to characterize voltage gating. As a simple example, we used the models to characterize the voltage gating of the homotypic Cx30 channel (Fig. 2*A*). First, we calculated the normalized conductance $g_n(V)$ from $G_{ss}(V)/G_i(V)$. The normalization here is performed against the $G_i(V)$ values at each voltage point according to the definition of g_n (see *Eq. 4*), different from the prior normalization of conductance to the single G_i at 0 mV for comparing data from different cell pairs. Because g_n reflects the P_o and is dimensionless, the normalization here also automatically takes into account the different coupling levels. We used the contingent model (*Eq. 8*) to fit the data and obtained gating parameters of $A = 0.116$ mV^{-1} and $V_o = 41.5$ mV for each voltage gate (Table 1). The g_{res} is 25% of the initial conductance, $g_{res} = 0.25$. The g_{max} is equal to the initial conductance, $g_{max} = 1.00$.

The calculated $P_{o,i}$ is 1.0 for the homotypic Cx30 channel (*Eq. 14*). However, the error margin of the parameters is strongly dependent on the precision of the experimental data. For example, single-channel measurements showed that $P_{o,i}$ of the homotypic Cx43 channel is ~0.8 (4, 8). However, the parameters obtained from fitting of the averaged macroscopic data of Cx43 gave $g_{res} = 0.29$ and $g_{max} = 1.00$, which result in

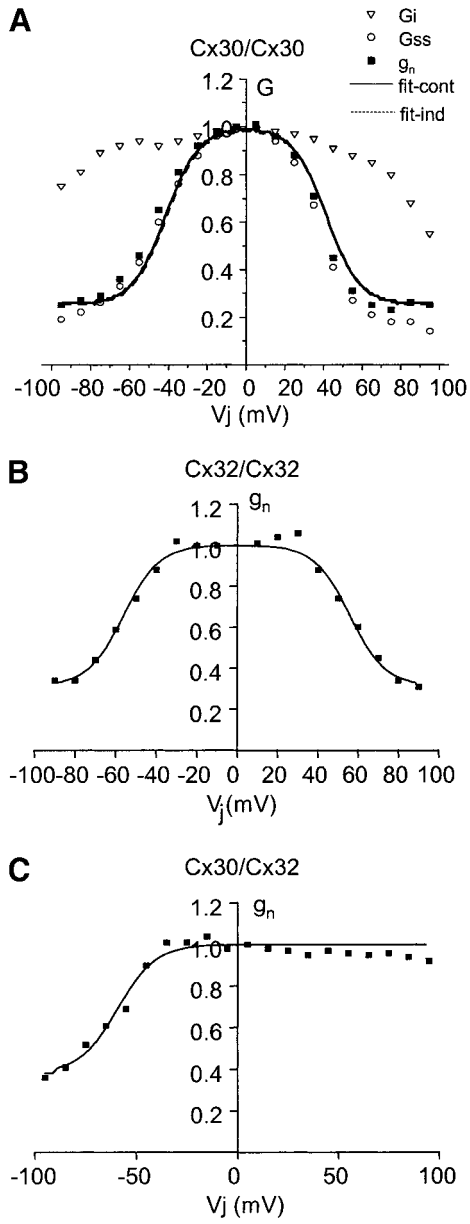

Fig. 2. Voltage gating of homotypic and heterotypic channels made of Cx30 and Cx32. *A*: conductances of homotypic Cx30/Cx30 channel are shown in G_i-V_j, G_{ss}-V_j, and normalized conductance (g_n)-V_j relationships. Values are averaged data from ≥17 cell pairs. The g_n-V_j relationship is fitted to contingent (solid line) and independent (dashed line) models. The 2 models yield identical fitting curves: solid and dashed lines are superimposed. Gating parameters from the 2 models also have the same value up to the 3rd decimal point (Table 1). *B*: g_n-V_j relationship of homotypic Cx32/Cx32 channel is well fitted to contingent (solid line) and independent (dashed line) models. The 2 models yield identical fitting curves: solid and dashed lines are superimposed. *C*: g_n-V_j relationship of heterotypic Cx30/Cx32 channel is also well fitted to contingent (solid line) and independent (dashed line) models. The 2 models yield identical fitting curves: solid and dashed lines are superimposed.

a calculated $P_{o,i}$ of 1.0 (Table 1). The apparent discrepancy in the $P_{o,i}$ values most likely arises from errors in the parameters. In the case of Cx43 data, the standard error of g_{res} is 0.08 and that of g_{max} is 0.03. The calculated $P_{o,i}$ should have a standard error of 0.2 (calculated by deriving the error of $P_{o,i}$ from that of G_{res} and G_{max} in *Eq. 14* using standard method). Therefore, the $P_{o,i}$ of 0.8 is within the error margin. We will not include the detailed statistics of fitting and error estimates, because we wish to focus on the basic principles and features of the model.

We also used the independent model (*Eq. 11*) to fit the data and obtained gating parameters of the same values up to the precision of data (Fig. 2*A*).

Because of the symmetry in homotypic channel gating, it is no surprise that the negative values $A = -0.116$ mV^{-1} and $V_o = -41.5$ mV also fit the voltage-gating profile of Cx30/Cx30. This raises the question of gating polarity. By convention, a connexon is deemed to have positive gating polarity if it closes at positive voltages referenced to its cytoplasmic side or to have negative gating polarity if it closes at negative voltages (2, 17, 30, 34). Gating polarity cannot be determined in homotypic channels because of the symmetry in voltage gating. Consequently, gating polarity can be determined only from heterotypic pairings (17) or between wild-type and mutant connexins (34). Application of this strategy (see DISCUSSION) leads to the assignment of positive gating polarity to Cx30. We calculate the equivalent gating charge and the transition energy of Cx30 in its homotypic channel as $Q = 3.0\ e$ and $U_o = 125$ meV (Table 1). These parameters for homotypic Cx30 channel gating are denoted Cx30(3.0 *e*, 125 meV) and defined as the reference value of Cx30.

DISCUSSION

Gating polarity. After the parameters for the two voltage gates in an intact gap junction channel are obtained, an immediate question arises: which gate belongs to which connexon hemichannel? In previous studies, investigators developed a method to match the gate to its host connexon. Stated simply, the two gates in heterotypic CxL/CxR channels are matched with CxL and CxR according to how closely the gating parameters resemble the reference values of CxL and CxR (22, 34). Here we propose a refinement of the formalism for this often loosely applied principle.

First, we suggest using the physical parameters Q and U_o, instead of the descriptive parameters A and V_o, as the basis for comparison. Because the physical parameters can be better related to the underlying molecular structure, they make a more meaningful comparison. Some investigators have already used equivalent gating charge to characterize gap junction voltage gating (22, 28, 34). Second, we suggest establishing a hierarchy with Q as the primary criterion and U_o as the secondary criterion for comparison. The reason for this is that docking interaction probably causes less change in Q than in U_o, because Q is mainly determined by the charged and polar residues in the gating domain, whereas U_o reflects the energy contribution associated with not only the gating charges but also the protein conformational change due to docking.

For example, the two voltage gates in the heterotypic Cx40/Cx37 channels have parameters gate$_{-V}$(10.5 *e*, 277 meV) and gate$_{+V}$(6.3 *e*, 124 meV) (Fig. 3, Table 1) for gating in the negative and positive voltage ranges, respectively. The reference value of Cx40 is Cx40(8.0 *e*, 276 meV) and that of Cx37 is Cx37(6.7 *e*, 110 meV) (Fig. 3, Table 1). With Q and U_o values for comparison, gate$_{-V}$ should be matched to Cx40 and gate$_{+V}$ to Cx37. Hence,

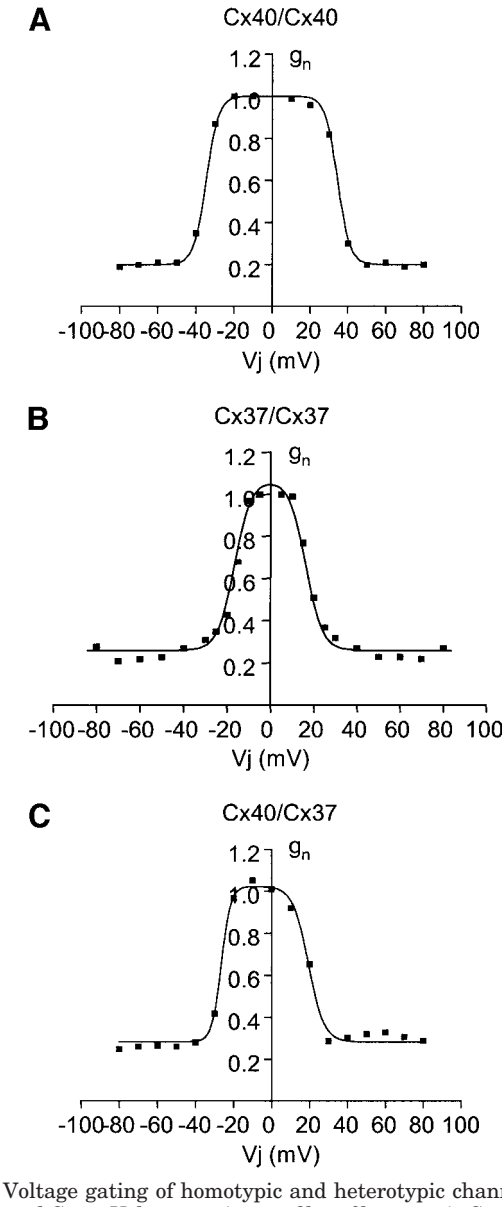

Fig. 3. Voltage gating of homotypic and heterotypic channels made of Cx37 and Cx40. Voltage-gating profiles of homotypic Cx40 channel (*A*), homotypic Cx37 channel (*B*), and heterotypic Cx40/Cx37 channel (*C*) are fitted to contingent or independent model. Symbols, averaged experimental data; lines, fitting curve from either model. Resulting voltage-gating parameters are listed in Table 1. In earlier publications (17, 22), homotypic Cx37 channel gating profile was shown as G_{ss} (normalized to G_i at 0 mV), instead of g_n ($g_n = G_{ss}/G_i$). G_{ss}-V_j relationship seemed best fitted to the sum of 2 Boltzmann functions; g_n-V_j relationship is best fitted to a single Boltzmann function.

the Cx37 gate closes at positive voltages referenced to its cytoplasmic side, whereas Cx40 channels close at negative voltages referenced to the Cx37 side, or in the positive voltage range referenced to its own side. Therefore, Cx37 and Cx40 have positive gating polarity, in agreement with that originally assigned by Hennemann et al. (17). We denote the voltage-gating parameters of the heterotypic Cx40/Cx37 channel as follows: Cx40(10.5 *e*, 277 meV)/Cx37(6.3 *e*, 124 meV).

Another simple example is Cx43/Cx45. The two gates in the heterotypic Cx43/Cx45 channels have the following parameters: gate$_{-V}$(2.3 *e*, 51 meV) and gate$_{+V}$(0.7 *e*, 89 meV) (Fig. 4, Table 1). The reference values are Cx43(1.5 *e*, 92 meV) and Cx45(2.8 *e*, 29 meV) (Fig. 4, Table 1). With the Q value as the first criterion, gate$_{-V}$ should be matched to Cx45 and gate$_{+V}$ to Cx43. Hence, the Cx45 gate closes at negative voltages referenced to its cytoplasmic side, whereas Cx43 channels close at positive voltages referenced to the Cx45 side, or in the negative voltage range referenced to its own side. Therefore, Cx45 and Cx43 have negative gating polarity. We denote their gating as Cx43(−0.7 *e*, 89 meV)/Cx45(−2.3 *e*, 51 meV).

In the heterotypic channels Cx40/Cx37 and Cx43/Cx45, the Q values of the two voltage gates are very different; hence, the gates can be assigned, using Q as the primary criterion, to their host connexons without much ambiguity. If the Q values of the two gates are similar, e.g., in Cx26/Cx50 (Table 1), the U_o values are used to assign the gates to their host connexons. In the case that the Q and U_o values of the two voltage gates in a heterotypic channel are similar, statistical evaluation of the difference in the parameter values would be necessary. First, the difference between the Q values should be tested for statistical significance. If they are insignificant, then the difference between the U_o values is tested. The convention and the objective of the "similarity principle" are to assign the two voltage gates to the two member connexons in a heterotypic channel in a way that minimizes the changes in Q (primary criterion) and U_o (secondary criterion).

The heterotypic Cx30/Cx32 channel presents an interesting case. Only the gate at negative voltages, gate$_{-V}$, can be determined; the gate at positive voltages, gate$_{+V}$, is absent in the voltage range of experimentation (Fig. 2*B*). Although it is possible that gating might occur at positive voltages outside the experimental voltage range, evidence has been presented that the gating polarity of Cx32 is negative (34). If this is the case, then Cx30 and Cx32 in the heterotypic Cx30/Cx32 channel close at negative voltages, while neither closes at positive voltages. Presumably, in the voltage range where both gates are partially closed, the measured conductivity should reflect the product of open probabilities for the two gates. This observation is consistent with the behavior of other heterotypic combinations of Cx32 with connexons of positive gating polarity, e.g., Cx26 (2) and Cx46 and Cx50 (36, 37), where the gate$_{-V}$ closely resembles a Cx32 gating profile.

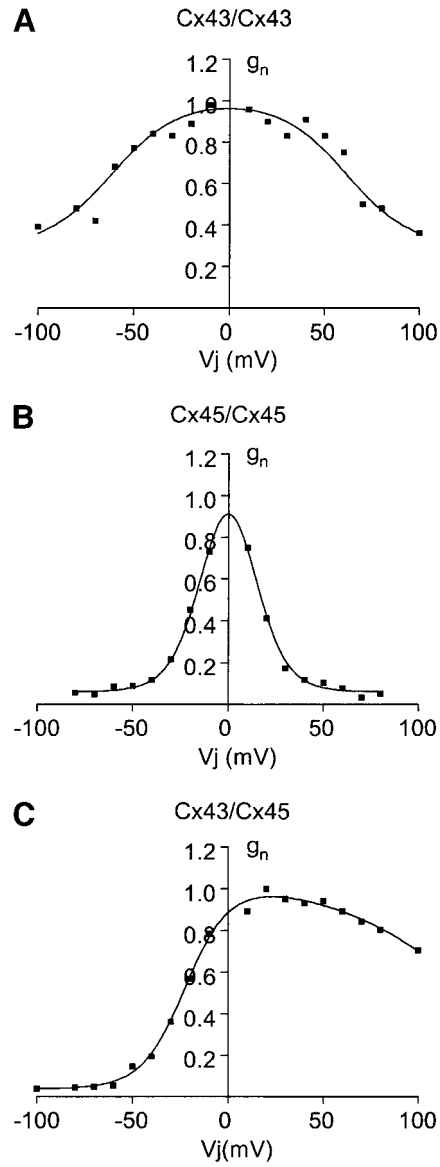

Fig. 4. Voltage gating of homotypic and heterotypic channels made of Cx43 and Cx45. Voltage-gating profiles of homotypic Cx43/Cx43 (*A*), homotypic Cx45/Cx45 (*B*), and heterotypic Cx43/Cx45 (*C*) channels are best fitted to contingent or independent model. Symbols, averaged experimental data; lines, fitting curve from either model. Resulting voltage-gating parameters are listed in Table 1. Homotypic Cx45/Cx45 channel demonstrates a clear case where initial conductance is smaller than maximum conductance. Only ~63% of the channels are open at the initial moment. Heterotypic Cx43/Cx45 channel profile clearly shows an "off-center peak."

Docking interaction between two member connexons in an intact channel. Two connexons dock through their extracellular loops to form an intact gap junction channel, although some connexon pairs are incapable of docking with each other to form functional channels (16, 36, 37). Docking interaction often introduces changes in the connexon voltage-gating characteristics (for summary see Refs. 5 and 12). Here we propose to measure the changes in the voltage gating of Cx*A* because of its heterotypic docking with Cx*B* as the difference between the gating parameters of Cx*A* in the

heterotypic Cx*A*/Cx*B* channel and the reference value of Cx*A*.

For example, the heterotypic Cx40/Cx37 channel has gating parameters Cx40(10.5 *e*, 277 meV)/Cx37(6.3 *e*, 124 meV). The reference values are Cx40(8.0 *e*, 276 meV) and Cx37(6.7 *e*, 110 meV). Hence, we calculate the docking interaction between Cx40 and Cx37 as follows: in Cx40, the equivalent gating charge is increased by 2.5 *e* (= 10.5 *e* − 8.0 *e*), and the transition energy is increased by 1 meV (= 277 meV − 276 meV); in Cx37, the equivalent gating charge is decreased by 0.4 *e,* and the transition energy is increased by 13 meV (Table 1). The above changes in the gating parameters of Cx40 and Cx37 serve to characterize the heterotypic docking interaction, in reference to the docking interactions of the homotypic channels.

The changes in the Q and U_o values lead to corresponding changes in the voltage-gating profile. The functional implication is that the larger the Q value, the more sensitive the gating in response to voltage change (steeper gating profile), and the larger the U_o value, the greater the voltage across the channel needed to close the gate. An increase of 25 meV in the U_o value causes an *e*-fold increase in the equilibrium constant between the open and closed gating states.

Table 1 lists the voltage-gating parameters of several representative connexon pairings. The homotypic "reference values" for nine of the known connexins (i.e., Cx26, Cx30, Cx30.3β, Cx32, Cx37, Cx40, Cx43, Cx45, and Cx50) are shown. Heterotypic pairings between positive gating connexins (Cx30/Cx26, Cx40/Cx37, Cx26/Cx30.3β, and Cx26/Cx50), negative gating connexins (Cx43/Cx45), and positive and negative gating connexins (Cx30/Cx32), as well as interactions between α-connexins (Cx40/Cx37 and Cx43/Cx45), β-connexins (Cx26/Cx30, Cx26/Cx30.3β, and Cx30/Cx32), and α- and β-connexins (Cx26/Cx50), are illustrated. The changes in the voltage-gating parameters of several connexon pairs from their homotypic docking interaction reveal that some heterotypic docking causes only slight changes in the voltage gating of member connexons, e.g., the heterotypic docking of Cx37 and Cx40. However, some heterotypic docking significantly alters the voltage gating of member connexons, as in the case of heterotypic docking of Cx26 with Cx50, Cx30.3β, or Cx50. We speculate that the extent of alteration in the connexon voltage gating due to docking is dependent on the rigidity of its docking domain relative to that of the partner.

In summary, the present model is a natural extension of the original S-H-B model (15, 28). We have added necessary complexity to model the asymmetric gating of a heterotypic channel, mainly by integrating the two voltage gates from the two hemichannel connexons. At the same time, we introduce three assumptions to circumscribe the complexity in a general model (35), so the present model can be used as a practical tool to fit the experimental data of macroscopic currents without too much ambiguity. The limitation of the model comes from its simplifying assumptions. The requirement of thermodynamic consistency should always hold true. The assumption of an independent or a contingent model provides a simple mathematical formula. The assumption of one open channel conductance and one residual conductance limits the number of independent parameters in the fitting equations, so the experimental data can be fitted without ambiguity. In principle, the above constraints limit the model application to the channels that have only one voltage gate on each hemichannel, one single-channel conductance, and one residual conductance. In practice, however, many known channels possess features that approximate these conditions and, therefore, can be characterized using the present model. For example, Cx43 has a fast voltage gating and a slower gating (1, 24). Because the fast gating happens within milliseconds, the slower gating (~100 times slower) can be easily separated from the former and characterized using this model. In another example, the single-channel conductance of Cx43 is seen as 60 pS in some cells and as 90 pS in others. However, for a given expression system, the Cx43 channel demonstrates only one dominant conductance level (21). Hence, the present model can be used to approximate the gating behavior. The voltage-gating profiles of all the channels listed in Table 1, except the heterotypic Cx43/Cx45 channel, demonstrate similar residual conductance levels at positive and negative voltage ranges. Therefore, the present model can apply to these channels. In the case of Cx43/Cx45, the voltage-gating profile shows that gate at the positive voltage range has not reached the residual conductance level within the experimental voltage range (Fig. 4*C*). Recently, using longer voltage steps, we found that the residual conductance is similar in positive and negative voltage ranges with a value very close to zero (unpublished data).

Thus this model does not apply to the channels with multiple single-channel conductance levels, with more than two voltage gates, or with two different residual conductance levels. Nor does the model attempt to describe the kinetic behavior of channels. The present model aims to describe the steady-state properties of the voltage gating at the level of macroscopic currents. The model sets consistent criteria to characterize the gating of heterotypic and homotypic channels in a comprehensive and intuitive way. The model also provides a practical formalism for fitting the voltage-gating profile over the entire voltage range, eliminating the previous need for data splicing. Hence, this model presents a useful tool for quantitatively characterizing the voltage gating of a population of gap junction channels.

We thank Dr. Bruce J. Nicholson for substantial input into the writing of the manuscript and for sharing the experimental data on Cx26, Cx30.3β, and Cx50; Dr. Thomas M. Suchyna for sharing the experimental data on Cx37/Cx40; and Drs. Leighton T. Izu and Edward G. Lakatta for comments on the manuscript.

Y. Chen-Izu was supported, in part, by National Cancer Institute Grant CA-480490 (to Bruce J. Nicholson) and by the Interdisciplinary Training Program in Muscle Biology, Department of Biochemistry and Molecular Biology, University of Maryland School of Medicine. A. P. Moreno was supported, in part, by National Heart, Lung,

and Blood Institute Grant HL-63969 and an Indiana University Research Venture Award.

REFERENCES

1. **Banach K and Weingart R.** Voltage gating of Cx43 gap junction channels involves fast and slow current transitions. *Pflügers Arch* 439: 248–250, 2000.
2. **Barrio LC, Suchyna T, Bargiello T, Xu LX, Roginski RS, Bennett MV, and Nicholson BJ.** Gap junctions formed by connexins 26 and 32 alone and in combination are differently affected by applied voltage. *Proc Natl Acad Sci USA* 89: 4220, 1992.
3. **Brink PR, Cronin K, and Ramanan SV.** Gap junctions in excitable cells. *J Bioenerg Biomembr* 28: 351–358, 1996.
4. **Brink PR, Ramanan SV, and Christ GJ.** Human connexin 43 gap junction channel gating: evidence for mode shifts and/or heterogeneity. *Am J Physiol Cell Physiol* 271: C321–C331, 1996.
5. **Bruzzone R, White TW, and Paul DL.** Connections with connexins: the molecular basis of intercellular signaling. *Eur J Biochem* 238: 1–27, 1996.
6. **Bukauskas FF and Peracchia C.** Two distinct gating mechanisms in gap junction channels: CO_2-sensitive and voltage-sensitive. *Biophys J* 72: 2137–2141, 1997.
7. **Bukauskas FF and Weingart R.** Voltage-dependent gating of single gap junction channels in an insect cell line. *Biophys J* 67: 613–625, 1994.
8. **Burt JM and Spray DC.** Single-channel events and gating behavior of the cardiac gap junction channel. *Proc Natl Acad Sci USA* 85: 3431–3434, 1988.
9. **Cao F, Eckert R, Elfgang C, Nitsche JM, Snyder SA, Hulser DF, Willecke K, and Nicholson BJ.** A quantitative analysis of connexin-specific permeability differences of gap junctions expressed in HeLa transfectants and *Xenopus* oocytes. *J Cell Sci* 111: 31–43, 1998.
10. **Chen-Izu Y, Spangler RA, and Nicholson BJ.** Opposing gates model for gap junction voltage-gating (Abstract). *Biophys J* 74: A317, 1998.
11. **Dahl E, Manthey D, Chen Y, Schwarz HJ, Chang YS, Lalley PA, Nicholson BJ, and Willecke K.** Molecular cloning and functional expression of mouse connexin-30, a gap junction gene highly expressed in adult brain and skin. *J Biol Chem* 271: 17903–17910, 1996. [Corrigenda. *J Biol Chem* 271: 26444, 1996.]
12. **Elfgang C, Eckert R, Lichtenberg-Frate H, Butterweck A, Traub O, Klein RA, Hulser DF, and Willecke K.** Specific permeability and selective formation of gap junction channels in connexin-transfected HeLa cells. *J Cell Biol* 129: 805–817, 1995.
13. **Foote CI, Zhu X, Zhou L, and Nicholson BJ.** The pattern of disulfide linkages in the extracellular loop regions of Cx32 suggests a model for the docking interface of gap junctions. *J Cell Biol* 140: 1187–1197, 1998.
14. **Goldberg GS, Lampe PD, and Nicholson BJ.** Selective transfer of endogenous metabolites through gap junctions composed of different connexins. *Nat Cell Biol* 1: 457–459, 1999.
15. **Harris AL, Spray DC, and Bennett MV.** Kinetic properties of a voltage-dependent junctional conductance. *J Gen Physiol* 77: 95–117, 1981.
16. **Hennemann H, Dahl E, White JB, Schwarz HJ, Lalley PA, Chang S, Nicholson BJ, and Willecke K.** Two gap junction genes, connexin 31.1 and 30.3, are closely linked on mouse chromosome 4 and preferentially expressed in skin. *J Biol Chem* 267: 17225–17233, 1992.
17. **Hennemann H, Suchyna T, Lichtenberg-Frate H, Jungbluth S, Dahl E, Schwarz J, Nicholson BJ, and Willecke K.** Molecular cloning and functional expression of mouse connexin40, a second gap junction gene preferentially expressed in lung. *J Cell Biol* 117: 1299–1310, 1992.
18. **Hermans MMP, Kortekaas P, Jongsma HJ, and Rook MB.** pH sensitivity of the cardiac gap junction proteins, connexin 45 and 43. *Pflügers Arch* 431: 138–140, 1995.
19. **Liu SG, Taffet S, Stoner L, Delmar M, Vallano ML, and Jalife J.** A structural basis for the unequal sensitivity of the major cardiac and liver gap junctions to intracellular acidification—the carboxyl tail length. *Biophys J* 64: 1422–1433, 1993.
20. **Moreno AP, Fishman GI, Beyer EC, and Spray DC.** Voltage-dependent gating and single channel analysis of heterotypic gap junction channels formed of Cx45 and Cx43. *Prog Cell Res* 4: 405–408, 1995.
21. **Moreno AP, Rook MB, Fishman GI, and Spray DC.** Gap junction channels: distinct voltage-sensitive and -insensitive conductance states. *Biophys J* 67: 113–119, 1994.
22. **Nicholson BJ, Suchyna T, Xu LX, Hammernick FL, Cao FL, Fourtner C, Barrio L, and Bennett MVL.** Divergent properties of different connexins expressed in *Xenopus* oocytes. *Prog Cell Res* 3: 3–13, 1993.
23. **Ramanan SV, Brinck PR, Varadaraj K, Peterson E, Schirmacher K, and Banach K.** A three-state model for connexin37 gating kinetics. *Biophys J* 76: 2520–2529, 1999.
24. **Revilla A, Castro C, and Barrio LC.** Molecular dissection of the transjunctional voltage dependence of connexin-32 and connexin-43 junctions. *Biophys J* 77: 1374–1383, 1999.
25. **Robinson SR, Hampson EC, Munro MN, and Vaney DI.** Unidirectional coupling of gap junctions between neuroglia. *Science* 262: 1072–1074, 1993.
26. **Rubin JB, Verselis VK, Bennett MV, and Bargiello TA.** Molecular analysis of voltage dependence of heterotypic gap junctions formed by connexins 26 and 32. *Biophys J* 62: 183–195, 1992.
27. **Simon AM and Goodenough DA.** Diverse functions of vertebrate gap junctions. *Trends Cell Biol* 8: 477–483, 1998.
28. **Spray DC, Harris AL, and Bennett MV.** Equilibrium properties of a voltage-dependent junctional conductance. *J Gen Physiol* 77: 77–93, 1981.
29. **Spray DC, White RL, Campos de Carvalho A, Harris AL, and Bennett MLV.** Gating of gap junction channels. *Biophys J* 45: 219–230, 1984.
30. **Suchyna TM, Xu LX, Gao F, Fourtner CR, and Nicholson BJ.** Identification of a proline residue as a transduction element involved in voltage gating of gap junctions. *Nature* 365: 847–849, 1993.
31. **Trexler EB, Bennett MV, Bargiello TA, and Verselis VK.** Voltage gating and permeation in a gap junction hemichannel. *Proc Natl Acad Sci USA* 93: 5836–5841, 1996.
32. **Unger VM, Kumar NM, Gilula NB, and Yeager M.** Three-dimensional structure of a recombinant gap junction membrane channel. *Science* 283: 1176–1180, 1999.
33. **Veenstra RD.** Size and selectivity of gap junction channels formed from different connexins. *J Bioenerg Biomembr* 28: 327–337, 1996.
34. **Verselis VK, Ginter CS, and Bargiello TA.** Opposite voltage gating polarities of two closely related connexins. *Nature* 368: 348–351, 1994.
35. **Vogel R and Weingart R.** Mathematical model of vertebrate gap junctions derived from electrical measurements on homotypic and heterotypic channels. *J Physiol (Lond)* 510: 177–189, 1998.
36. **White TW, Bruzzone R, Wolfram S, Paul DL, and Goodenough DA.** Selective interactions among the multiple connexin proteins expressed in the vertebrate lens: the second extracellular domain is a determinant of compatibility between connexins. *J Cell Biol* 125: 879–892, 1994.
37. **White TW, Paul DL, Goodenough DA, and Bruzzone R.** Functional analysis of selective interactions among rodent connexins. *Mol Biol Cell* 6: 459–470, 1995.